9 Emerging Methodologies for Turbulence Characterization in River Dynamics Study

Harinarayan Tiwari, Amir Khan, and Nayan Sharma

Abstract

River engineering study consists of large variation in time and spatial scales. Timescale of river varies from years to second, and, similarly, the variation of spatial scales is from kilometre to millimetre. Spatial scales can be divided into river basin scale and hydraulic scale, and temporal scale can be divided into hydrological, hydraulic and turbulence. Each spatio-temporal scale has fixed contextual uses. In general, turbulence plays the most key role with respect to the influences that rivers have on their channels and beds. Turbulent flows are characterized by asymmetrical patterns, irregular behaviour and the existence of various spatio-temporal scales. To extract better turbulence events and flow structure using point velocity measurements (Eulerian approach) in river, we are proposing generalized three-dimensional octant events instead of conventional two-dimensional quadrant events. Beyond that, we characterize the transitional probability of octant event occurrence in the case of unsteady flow condition. In the field, there is the assumption of steadiness of the flow under high unsteady conditions. Basically, river discharges and all the associated processes are physically unsteady, and river channel flows are typically non-uniform. In this chapter we are mainly discussing the new emerging methodological aspects to characterize the river turbulence using state-of-the-art technology. In this chapter, some of the major issues and developments linked with river dynamics and turbulence study have also been discussed with two case studies. The case studies have been presented and discussed using experimental data and their interpretation in light of river dynamics. The study has significant importance because the turbulent motion is the natural state of river engineering problems.

H. Tiwari (✉) • A. Khan • N. Sharma
Department of Water Resources Development and Management, Indian Institute of Technology Roorkee, Roorkee, Uttarakhand, India
e-mail: haribit31@outlook.com

N. Sharma (ed.), *River System Analysis and Management*, DOI 10.1007/978-981-10-1472-7_9

9.1 Introduction

River dynamics is subject of infinite opportunity with multidimensional faces (Fig. 9.1). Considering river as one of the important and limited source of freshwater, it is our prime duty to capture state-of-the-art approaches for the river science research. Rivers are natural open channels, draining water from the land. Rivers are auto-shaped channels in which channel dimensions, outline, slope and bed material character are adjusted through scouring and deposition of the unbalanced sediments through which they flow. The sediment transport rate depends not only on water discharge but also on channel slope, morphology and bed characteristics (Church and Ferguson 2015). So, channel system state and process are connected by feedback loops. Despite increasing appreciation of the potential of turbulence on sediment and momentum transport, key knowledge gaps exist in relation to turbulent events for sediment dynamics at micro-scales.

9.2 Multiple Scales in Rivers

Studies of river engineering are characterized by many scales of time and space (Fig. 9.2). The river scales vary from years to second in time and kilometre to millimetre in length (Church 1995; Helder and Ruardij 1982; Whipple and Tucker 1999). A viable theory of river science research must accommodate a variety of processes that occur at diverse scales. Interlinking between different scales of the processes requires enormous amount of quality data derived from the field and laboratory studies. The data quality and their

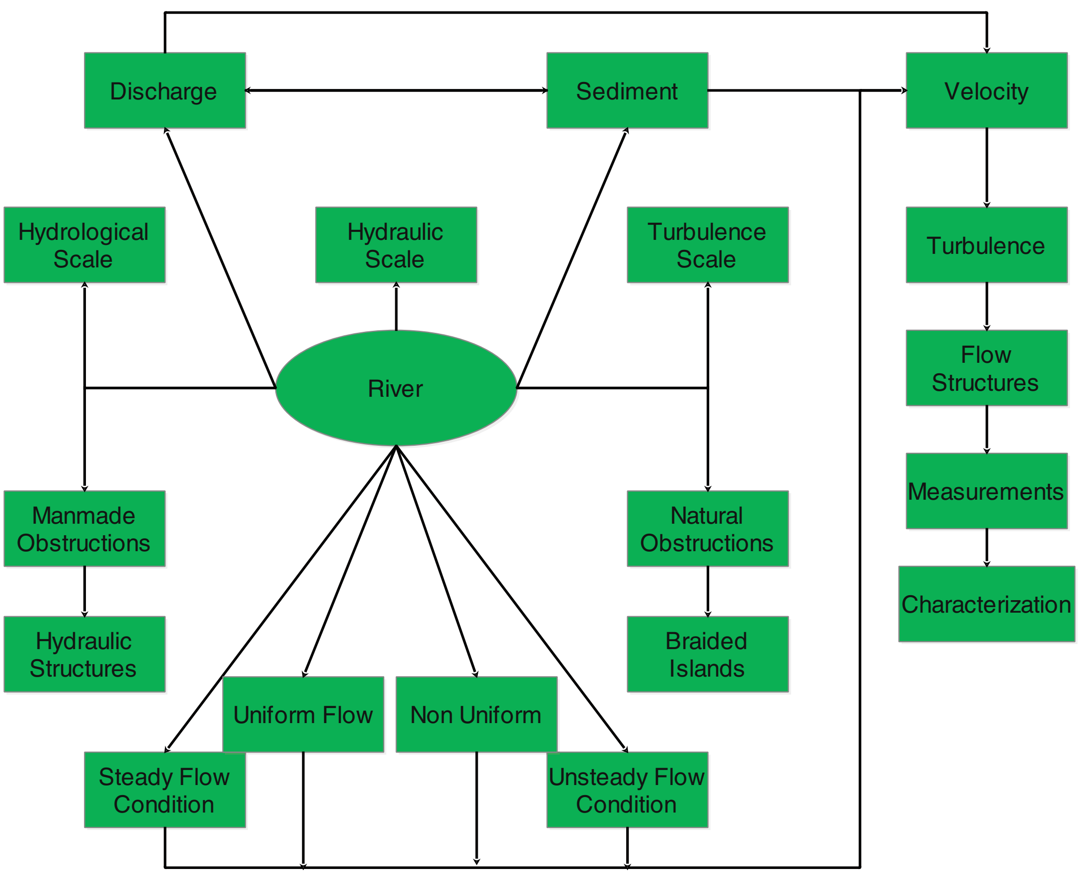

Fig. 9.1 River and some underlying components

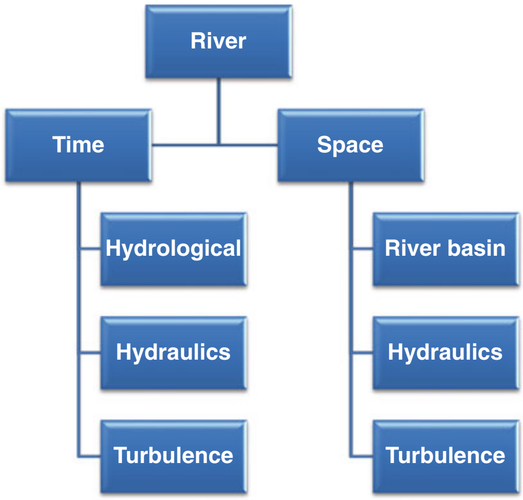

Fig. 9.2 Multiple scales for river science research

extraction are very much location specific, so the development of general river model based on multiple theoretical aspects is the major challenge for river engineers.

9.2.1 Hydrological Scale

The hydrological timescale of the river varies from years to hour which depends on the parameters of analysis. One concept of dealing with variability over many orders of magnitude is the notion of characteristic scales. The idea of a characteristic scale is that instead of dealing with a spectrum of lengths and times, one adopts a typical length and time that are representative of a particular process (Fig. 9.3). Often a

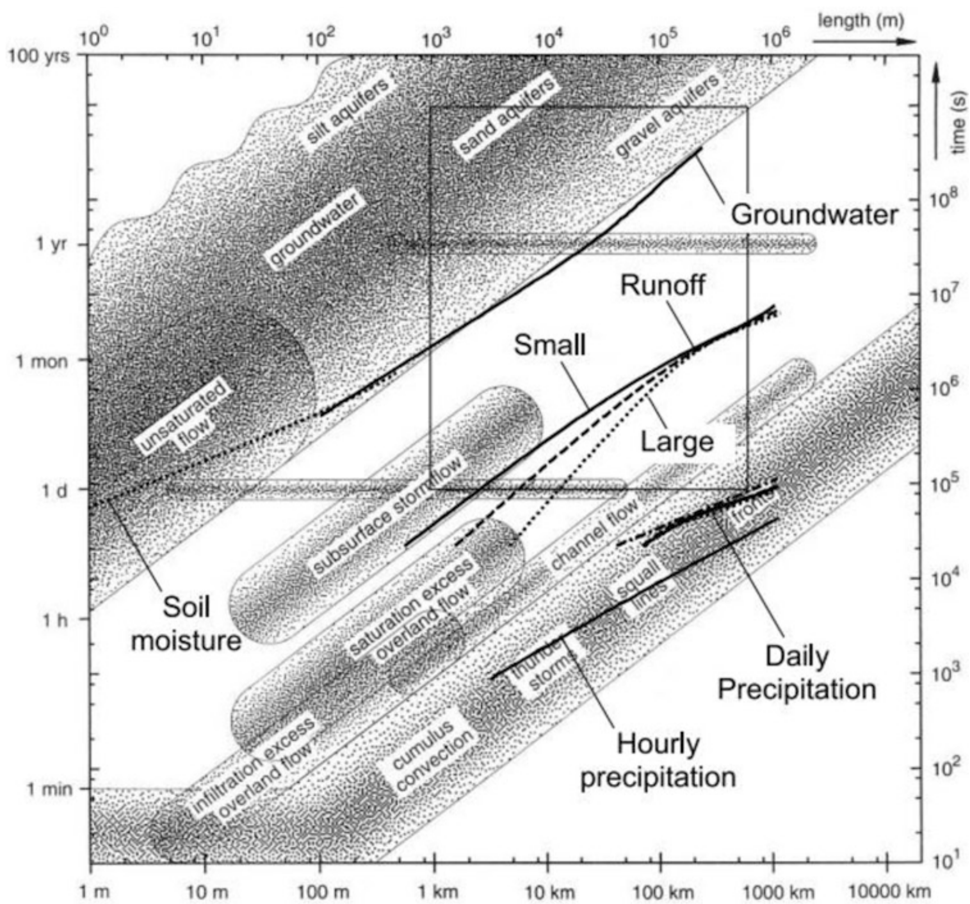

Fig. 9.3 Schematic relationship between spatial and temporal process scales in hydrology (Blöschl and Sivapalan 1995; Seyfried and Wilcox 1995)

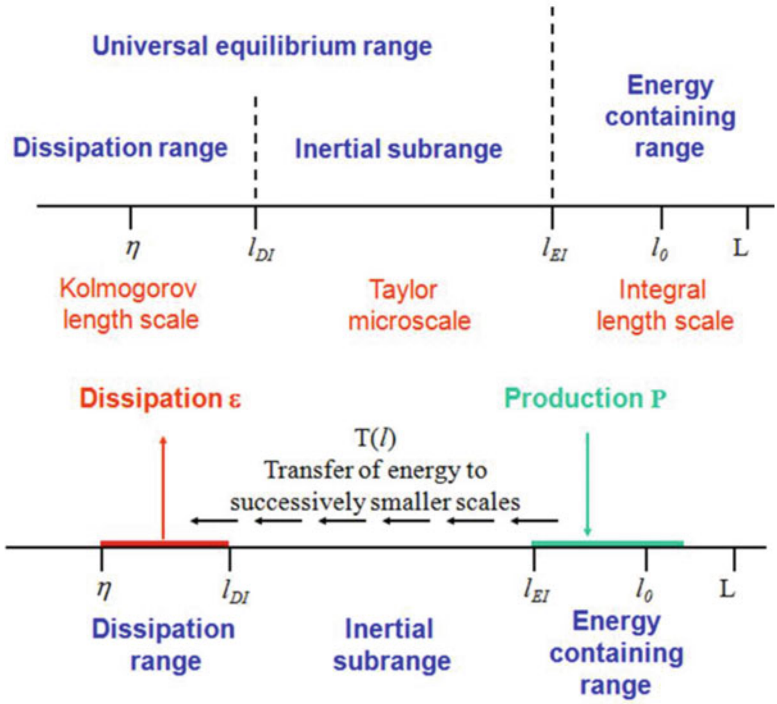

Fig. 9.4 Turbulence scale in hydraulics

characteristic scale is an order of magnitude figure, given as an integer power of ten, rather than a precise number.

9.2.2 Hydraulic Scale

Till date, there is no clear-cut discrimination between different timescales and space scales of river. Assumptions vary with the types of the problem and scope of the studies. Under basic assumptions, hydraulic timescale may be considered to be hours to second.

9.2.3 Turbulence Scale

According to Richardson, 'Big whirls have little whirls which feed on their velocity; and little whirls have lesser whirls, and so on to viscosity in the molecular sense' (Richardson 1921). The smallest known scale is the Kolmogorov scale under the dissipation range. At integral length scale, there is the production of energy by movement of fluid particle and it dissipates at finer scales (Fig. 9.4).

9.3 Turbulence

Turbulence appears in the channel when inertial forces dominate over viscosity forces in a flow, which means that the Reynolds number evaluating the relative strength of these two forces must exceed a certain threshold (Bradshaw 2013). The measurement and characterization of turbulence is certainly important due to its intrinsic association with sediment transportation, suspension and deposition (Gordon 1975). As any flow in river has three dimensions, so three-dimensional flow structure characterizations add an improvement to sediment entrainment and transport mechanism (Keshavarzi and Gheisi 2006; Mianaei and Keshavarzi 2008). Bursting events and their transitional probability occurrence help to extract better information on flow mechanism for three-dimensional numerical model developments. In the three-dimensional bursting events, there is consideration of lateral velocity in concurrence with longitudinal and vertical velocity simultaneously. In context of four basic bursting events, addition of lateral velocity makes it three dimensional (internal and external). Flow structures in environmental turbulent flows contain a significant part of the turbulent energy. Hence, they are important for momentum exchange as well as mixing and scalar and sediment transport (Keylock et al. 2005, 2014; Nepf and Vivoni 2000). The results of bursting events (quadrant and octant) add to understanding of the hydrodynamics of sediment transport mechanism and may be used for the development of better parameterizations of small-scale processes for application in large-scale studies under different hydraulic conditions. In addition to the complexity of the near-bed flow field, there has been widespread recognition of the need to go beyond Reynolds stress formulations in order to understand the interaction between turbulence and sediment entrainment (Keylock et al. 2014; Sharma and Tiwari 2013; Tiwari and Sharma 2015a, b). In the light of importance of turbulence bursting events, characterization of it under several natural conditions is needed. This chapter presents the study related to natural river condition under laboratory investigations. In the first part of the study, attempt has been made to derive the character of bursting events (quadrant and octant) under quasi-steady and unsteady flow conditions. In the second part of the study, the authors explored connection between the bed scouring/depositions features and bursting events under braided river laboratory model.

9.4 Case Study: Bursting Events for Quasi-steady and Unsteady Flow

Open channel flow in the nature is generally unsteady and assumed to be steady for estimation ease. The effect of unsteadiness in open channel has been continued as critical area of hydraulic research due to its wide field applications. Bursting events (quadrant and octant) have specific features depending on type of flow along with their hydraulic conditions. Transition probability calculates the occurrence of specific event after another event. The one-step transition probability is the probability of transitioning from one state to another in a single step and also termed as first-order Markov chain process. This study estimates the transition probability matrix of bursting events for the case of steady and unsteady flows. The transition probability matrix has been calculated using first-order Markov chain process. Significant change has been observed for the transition probabilities under steady and unsteady flow condition.

9.4.1 General

Flow is defined as steady when the flow parameters (i.e. discharge, depth) are constant over time span. Presumption of time span may vary according to the needs of the study. In nature, no open channel flow can be considered as purely steady. Quasi-steady is the state where unsteady flow over certain time interval can be assumed as steady. Nearly all geophysical flows, including open channel flows, are also turbulent. Bursting events are principal component of turbulent events. The coherent structures related with the bursting process are random in space and highly three dimensional, and their distinctive form and development have been hard to account and model in particular terms. Unsteady flow itself is very complex and an intensive area for a hydraulic researcher. Bursting events, especially quadrant events under quasi-steady flow, have relatively more literature than in unsteady flow. Quadrant events have been studied extensively along with Reynolds stress. The effects of the turbulent events on the sediment entrainment, transport and deposition have been comprehensively considered by the researchers. Literature review indicates that the main focus of bursting events is centred on two dimensional by considering two velocity components (u and w), where u is longitudinal velocity and w is the vertical velocity. Availability of high-quality velocity measuring instruments (i.e. acoustic Doppler velocimeter (ADV), laser Doppler velocimeter, etc.) has been deployed for observation of the three-dimensional velocity components. So, the combination of turbulent events with unsteadiness presents large complexities and needs experimental investigation.

9.4.2 Methodology

The bar chart (Fig. 9.5) has been presented to show the basic steps for first case study. The number of samples has been collected on very higher side (90,000). The experimental design was kept simple as shown in Fig. 9.6. For the first two conditions (E1 and E2 – Table 9.1), flow parameters (average discharge, average velocity, average depth, etc.) have been kept constant, while variation comes into picture for the third experimental condition (E3 – Table 9.1).

For each case, the total number of velocity samples has been taken equal. There are five general steps, which have been held during this study. It includes laboratory set-up, data collection, data modification, bursting events and then estimation of transition probability matrix.

9.4.3 Experimental Set-Up

The experimental study was conducted in the controlled open channel of the river engineering laboratory (Department of Water Resource Development and Management, Indian Institute of Technology, Roorkee, India). The channel is about 3 m long and 0.5 m wide. Figure 9.6 shows the L-section of the channel. The velocity measurements were taken at the mid of the channel from the channel bed using an acoustic Doppler velocimeter (ADV). ADV is a competent instrument for conducting turbulence study. SonTek 16 MHz ADV has been used to take

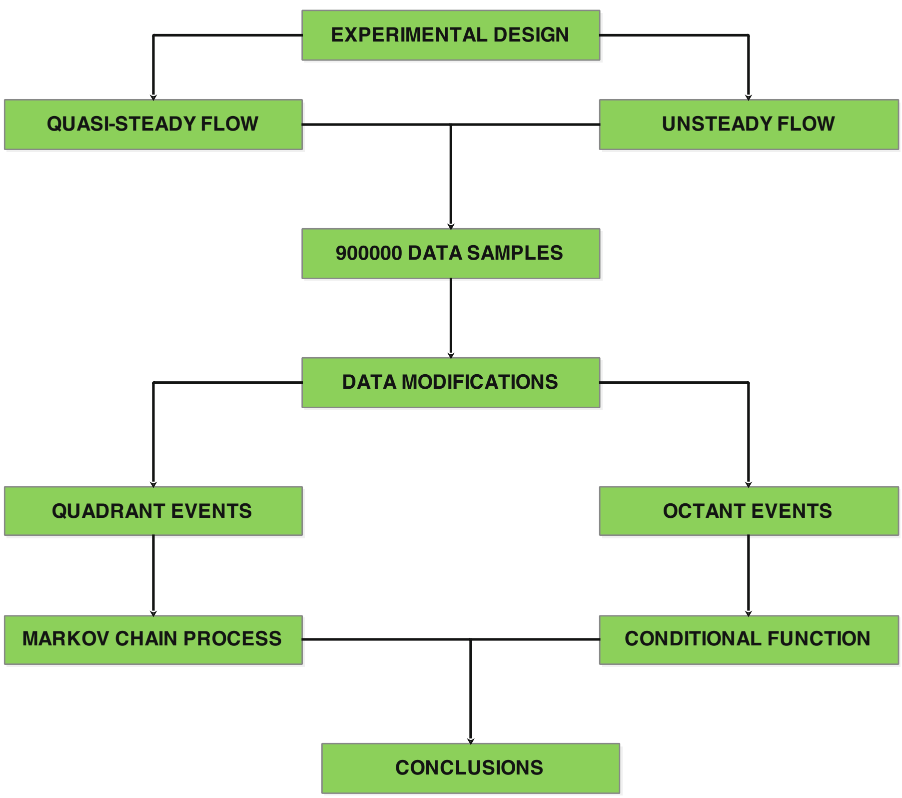

Fig. 9.5 Methodological charts for the case study

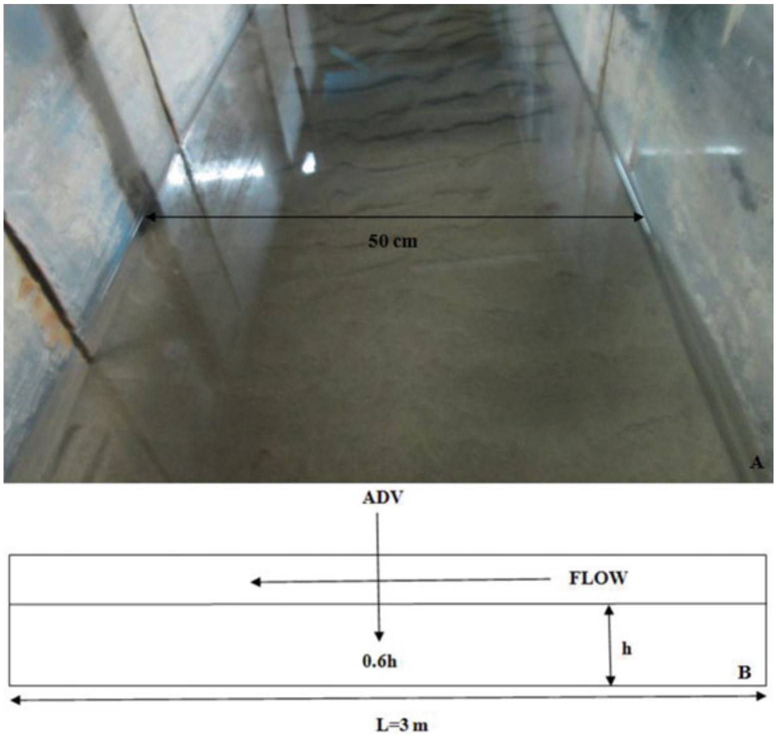

Fig. 9.6 (**a**) Cross section of experimental flume and (**b**) schematic diagram of L-section

Table 9.1 Experimental condition for case study 1

Experimental condition	Discharge (cc/s)	No. of velocity samples	Type of flow
E1	6055	90,000	Quasi-steady
E2	8400	90,000	Quasi-steady
E3	4670–9550	90,000	Unsteady

Table 9.2 Bursting events in *uw* plane

Sign of fluctuating velocities			
u'	w'	Quadrant events	Quadrant
+	+	Outward interaction (OI)	1
−	+	Ejection (EJ)	2
−	−	Inward interaction (II)	3
+	−	Sweeps (SW)	4

velocity measurements. Table 9.1 presents discharge variations for the experimental conditions, which have been considered in this part of study.

9.4.4 Theory of Bursting Events

Kline et al. (1967) divided two-dimensional bursting events into four-part (outward interaction, ejection, inward interaction and sweep) events based on longitudinal and vertical velocities (Table 9.2). Results of Kline et al. (1967) evaluate sweep and ejection events as important among the four bursting events on sediment motion (Kline et al. 1967). Reynolds shear stress is also affected by the occurrence of bursting events.

9.4.4.1 Bursting Events (Quadrant Events)

Bursting event research has continued using generally two-dimensional velocities (u and w). The study can be extended to analogous events (Table 9.3) in the transverse plane (v and w) and horizontal plane (u and v) to extract better information and their effect. Estimation of probability of occurrence (in %) has been carried out using Eq. (9.1) for every time series:

$$Q_k = \frac{\text{Number of event in } k\text{th quadrant } (k = 1 \text{ to } 4)}{\text{Total number of events } (N)} \times 100 \quad (9.1)$$

9.4.4.2 Theory of Transitional Probability

The probability based on the change of state with respect to time can be termed as transitional probability. For any time series having set of events, there are the chances of occurrence of any particular event after the other events. Q_{1-1} can be defined as the probability of occurrence of first quadrant events after first quadrant event. In this case where we have four sets of events (quadrant events), there is estimation of 4 × 4 matrix of transitional probability (T_{px}) of random (x) time series (Eq. 9.2):

$$T_{px} = \begin{bmatrix} Q_{1-1} & Q_{1-2} & Q_{1-3} & Q_{1-4} \\ Q_{2-1} & Q_{2-2} & Q_{2-3} & Q_{2-4} \\ Q_{3-1} & Q_{3-2} & Q_{3-3} & Q_{3-4} \\ Q_{4-1} & Q_{4-2} & Q_{4-3} & Q_{4-4} \end{bmatrix} \quad (9.2)$$

9.4.4.3 Results and Discussions

Transitional probability of bursting events using Eq. 9.1 has been estimated for three experimental conditions mentioned above (Table 9.1). It is estimated for all three planes (uw, uv and vw) under every experimental condition (Tables 9.4, 9.5 and 9.6).

Table 9.3 Analogous bursting events (quadrant events)

Sign of fluctuating velocities		Quadrant
v'	w'	
+	+	1
−	+	2
−	−	3
+	−	4
u'	v'	
+	+	1
−	+	2
−	−	3
+	−	4

Table 9.5 Transitional probabilities of quadrant events in horizontal plane (uv)

Expt. condition		$Q1$	$Q2$	$Q3$	$Q4$
E1	$Q1$	28.37	25.17	21.24	25.22
	$Q2$	23.26	30.02	24.66	22.06
	$Q3$	20.88	26.11	27.67	25.34
	$Q4$	24.50	22.22	23.50	29.78
E2	$Q1$	27.72	23.86	23.17	25.25
	$Q2$	24.91	25.93	25.81	23.35
	$Q3$	22.82	25.87	27.74	23.56
	$Q4$	24.87	23.46	25.46	26.22
E3	$Q1$	44.57	15.58	10.92	28.92
	$Q2$	15.15	37.95	32.42	14.49
	$Q3$	11.10	33.36	39.41	16.13
	$Q4$	28.35	14.40	15.70	41.55

Table 9.4 Transitional probabilities of quadrant events in vertical plane (uw)

Expt. condition		$Q1$	$Q2$	$Q3$	$Q4$
E1	$Q1$	26.08	21.93	23.75	28.24
	$Q2$	22.25	26.21	27.69	23.85
	$Q3$	23.47	27.91	26.58	22.04
	$Q4$	26.32	23.23	23.12	27.33
E2	$Q1$	27.00	25.22	24.33	23.45
	$Q2$	23.74	27.11	27.38	21.77
	$Q3$	23.88	23.70	27.29	25.13
	$Q4$	26.80	22.90	23.39	26.90
E3	$Q1$	34.60	23.75	15.13	26.51
	$Q2$	22.13	44.77	20.58	12.52
	$Q3$	13.66	25.95	41.15	19.24
	$Q4$	22.02	14.25	24.67	39.06

Table 9.6 Transitional probabilities of quadrant events in transverse plane (vw)

Expt. condition		$Q1$	$Q2$	$Q3$	$Q4$
E1	$Q1$	22.42	25.43	20.99	31.17
	$Q2$	19.50	29.03	23.85	27.63
	$Q3$	20.15	31.26	22.47	26.12
	$Q4$	22.88	26.86	20.11	30.15
E2	$Q1$	26.47	24.46	23.57	25.50
	$Q2$	25.56	26.59	23.89	23.96
	$Q3$	23.27	25.39	27.12	24.22
	$Q4$	24.80	23.76	25.87	25.56
E3	$Q1$	33.45	31.62	14.07	20.85
	$Q2$	26.48	34.83	19.01	19.68
	$Q3$	14.81	21.51	33.21	30.46
	$Q4$	19.25	20.25	27.29	33.20

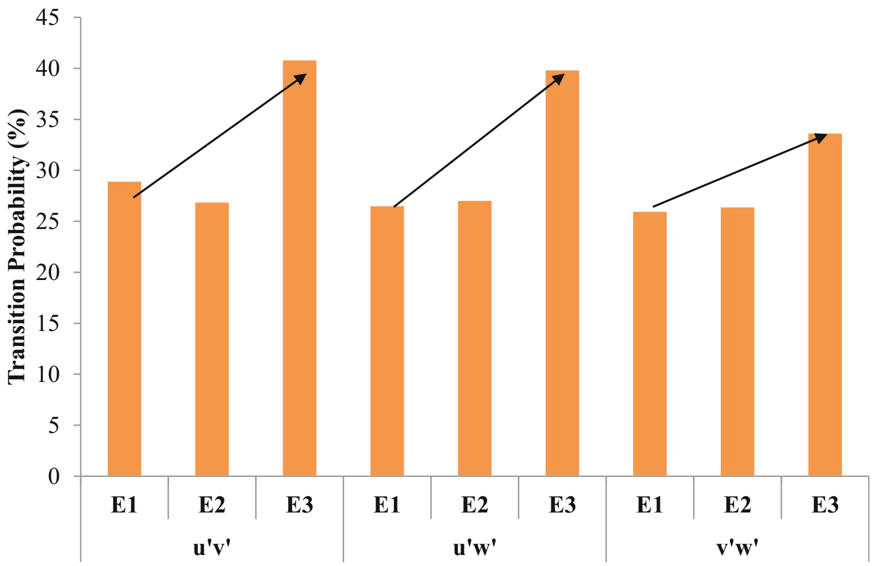

Fig. 9.7 Average diagonal transitional probabilities of quadrant events

The detailed analysis of Tables 9.4, 9.5, and 9.6 extracts the very notable point that at every plane, average probability of occurrence of diagonal event has been increasing under unsteady-state conditions (Fig. 9.7). The results also reveal that the effect of unsteadiness is maximum in horizontal plane (*uv*) and minimum in transverse plane (*vw*). Although this result may not be universal, but it can easily bring out some noticeable point that the contribution of unsteadiness is not similar in every plane, as in the case of steady flow.

9.4.5 Three-Dimensional Bursting Events (Octant Events)

Ali Reza Keshavarzi proposed a method of three-dimensional octant analysis, and it enables to take the effect of secondary flow (Keshavarzi and Gheisi 2006). As any flow in open channel has three dimensions, so three-dimensional bursting events may add an improvement to sediment entrainment and transport mechanism (Tiwari and Sharma 2014). In the three-dimensional bursting events, there is the consideration of lateral velocity in concurrence with longitudinal and vertical velocity simultaneously. In the context of four basic bursting events, addition of lateral velocity makes it three dimensional (internal and external – Table 9.7). Internal element of any of the event contributes into main flow domain and external element out to flow domain. Octant events and their transitional probabilities have been estimated using Eqs. 9.3 and 9.4:

$$O_k = \frac{\text{Number of events in } k\text{th octant } (k = 1 \text{ to } 8)}{\text{Total number of events } (N)} \times 100 \qquad (9.3)$$

$$T_{px} = \begin{bmatrix} O_{1-1} & O_{1-2} & O_{1-3} & O_{1-4} & O_{1-5} & O_{1-6} & O_{1-7} & O_{1-8} \\ O_{2-1} & O_{2-2} & O_{2-3} & O_{2-4} & O_{2-5} & O_{2-6} & O_{2-7} & O_{2-8} \\ O_{3-1} & O_{3-2} & O_{3-3} & O_{3-4} & O_{3-5} & O_{3-6} & O_{3-7} & O_{3-8} \\ O_{4-1} & O_{4-2} & O_{4-3} & O_{4-4} & O_{4-5} & O_{4-6} & O_{4-7} & O_{4-8} \\ O_{5-1} & O_{5-2} & O_{5-3} & O_{5-4} & O_{5-5} & O_{5-6} & O_{5-7} & O_{5-8} \\ O_{6-1} & O_{6-2} & O_{6-3} & O_{6-4} & O_{6-5} & O_{6-6} & O_{6-7} & O_{6-8} \\ O_{7-1} & O_{7-2} & O_{7-3} & O_{7-4} & O_{7-5} & O_{7-6} & O_{7-7} & O_{7-8} \\ O_{8-1} & O_{8-2} & O_{8-3} & O_{8-4} & O_{8-5} & O_{8-6} & O_{8-7} & O_{8-8} \end{bmatrix} \quad (9.4)$$

9.4.5.1 Results and Discussions

Results of octant events (Fig. 9.8) show some basic intrinsic relationship between octant events. It shows that there is positive intimacy between internal outward events ($O1$) and external inward events ($O6$). It also presents the similar positive intimacy among external outward interaction ($O2$), external ejection ($O4$)

Table 9.7 Three-dimensional bursting events (octant events)

SL no.	Sign of fluctuating velocities u'	v'	w'	Octant events
1	+	+	+	Internal outward interaction (IOI)
2	+	−	+	External outward interaction (EOI)
3	−	+	+	Internal ejection (IEJ)
4	−	−	+	External ejection (EEJ)
5	−	+	−	Internal inward interaction (III)
6	−	−	−	External inward interaction (EII)
7	+	+	−	Internal sweeps (ISW)
8	+	−	−	External sweeps (ESW)

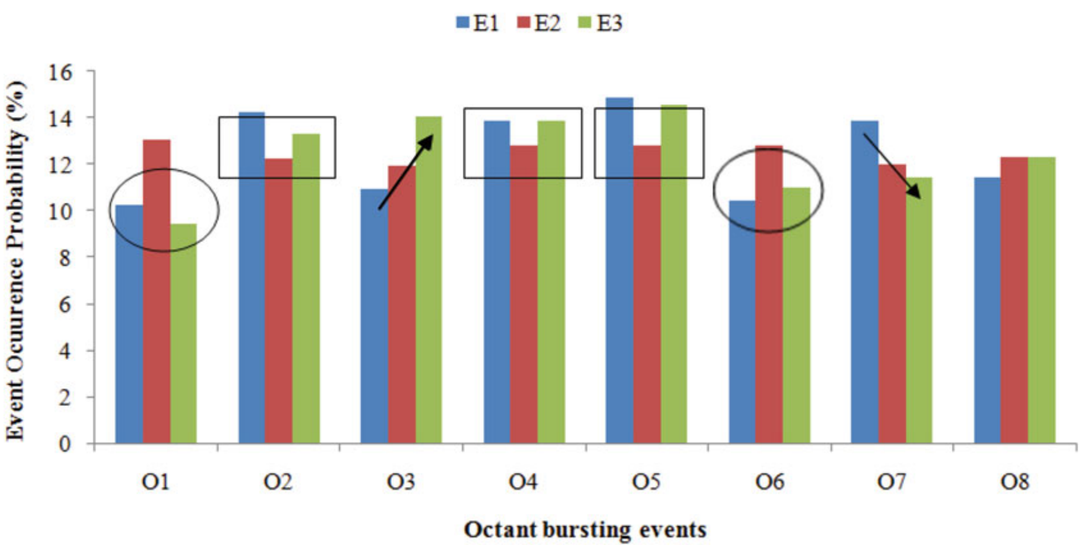

Fig. 9.8 Octant events under different experimental conditions

Table 9.8 Transitional probabilities of octant events for condition E1

11.66	14.06	10.37	11.72	14.73	9.56	16.41	11.49
10.83	15.25	9.49	12.43	13.89	9.86	15.23	13.01
10.50	14.18	10.59	12.70	15.00	10.13	14.76	12.13
10.05	14.10	10.71	13.37	15.09	10.65	14.06	11.97
10.08	13.80	11.22	13.72	15.44	10.58	13.77	11.40
9.99	13.93	11.21	14.17	15.31	10.71	13.37	11.31
10.27	13.92	11.16	13.85	15.15	10.46	13.89	11.30
10.28	14.25	10.96	13.88	14.87	10.41	13.91	11.45

Table 9.9 Transitional probabilities of octant events for condition E2

14.88	12.68	12.27	12.00	12.40	11.61	12.82	11.34
14.24	12.76	12.31	12.91	12.48	11.85	11.93	11.52
13.68	12.27	12.60	12.94	13.01	12.33	11.85	11.32
13.28	12.11	12.74	13.42	13.23	12.60	11.49	11.13
13.20	12.01	12.41	13.08	13.27	12.79	11.75	11.48
12.91	11.97	12.25	13.07	13.28	13.04	11.72	11.76
13.09	12.09	12.13	12.83	13.04	12.83	11.94	12.04
13.07	12.27	11.95	12.78	12.83	12.79	11.98	12.33

Table 9.10 Transitional probabilities of octant events for condition E3

16.48	18.73	14.04	10.75	9.37	5.29	13.88	11.46
14.55	20.05	12.09	11.66	9.04	6.09	12.97	13.55
13.12	16.97	16.88	15.25	10.40	6.42	10.55	10.40
11.74	15.98	17.97	17.36	10.85	7.29	9.37	9.43
10.51	14.21	17.06	16.30	13.66	9.46	9.41	9.40
9.65	13.36	16.21	15.98	14.79	11.06	9.26	9.69
9.72	13.31	15.15	14.78	14.73	10.91	10.55	10.86
9.47	13.31	14.06	13.87	14.55	11.02	11.43	12.29

and internal inward interaction ($O5$), while internal ejection ($O3$) and internal sweep ($O7$) have been found to be opposite in relationship. Increase in one event causes decrease in other event for all three considered experimental conditions.

Transitional probability matrix (Eq. 9.4) has been estimated using first-order Markov chain process for all three experimental conditions (Tables 9.8, 9.9 and 9.10).

To get the insight of the findings from the transitional probability matrix, average of column matrix (Fig. 9.9) and average of diagonal matrix (Fig. 9.10) have been plotted for each experimental condition.

9.4.6 Comparison Between Quadrant and Octant Analysis

Pattern of average diagonal probability has been found to be the same from quadrant and octant event analysis (Figs. 9.7 and 9.10). The average contribution of diagonal events from steady to unsteady is increasing for both the cases (quadrant and octant). Magnitude of increment has been found different in the different planes for two-dimensional quadrant analyses. For horizontal (uv) and vertical (uw) planes, the increment of average diagonal probability for unsteady flow has been estimated around 46–48 % in comparison with steady flow. The same was found to be

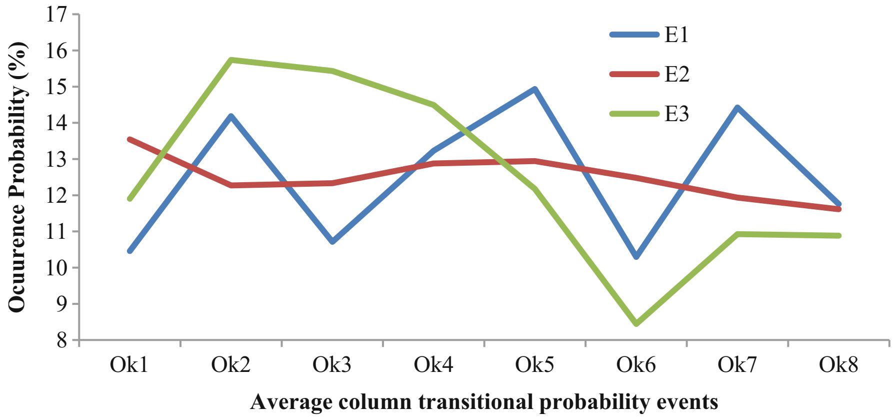

Fig. 9.9 Plot of average column transitional matrix for three experimental conditions (E1, E2 and E3)

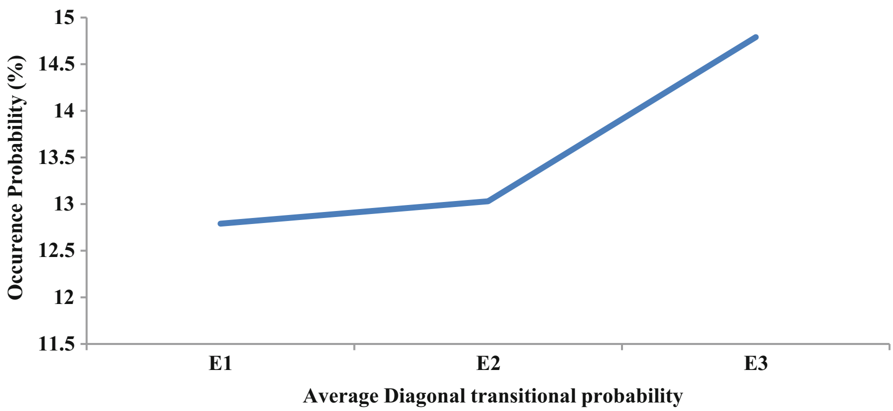

Fig. 9.10 Plot of average diagonal transitional matrix for three experimental conditions (E1, E2 and E3)

around 28 % in the transverse plane (*vw*) (Tables 9.4, 9.5 and 9.6). But in the case of three-dimensional event analysis (octant event), it was found that average diagonal contribution in unsteady flow is increased by 14 % compared to the steady flow conditions. It also shows that there is some factor which relate the events in isolation (three different quadrant events at different planes) and events occur simultaneously (octant events). Indeed it is of greater need to approximate the factor which may transfer the two-dimensional analysis to three-dimensional analysis.

9.4.7 Case Study 2: Bursting Events Under Braiding River Condition

A braided river is a river with a number of smaller channels, branched by islands. The islands may be small or large and temporary or permanent (Fig. 9.11).

9.4.7.1 General

River braiding usually occurs in the rivers having variable discharge with sufficient amount of sediment. Braided channel configuration usually forms on rivers with variable flow (wet and dry

Fig. 9.11 Braided Brahmaputra River in the upstream of Guwahati (India) (Ref: Google Earth)

season or snow melt season) and high quantities of sediment load. When a river flow is at maximum discharge, it is able to transport most of its loads. However, when the discharge falls along with the velocity (i.e. energy or power to carry sediment) of the river, deposition starts to take place.

Braided rivers comprise numerous, shifting channels that widen and become more numerous in response to increased river discharge. Factors which are directly involved in the braiding process of river are as follows:

1. Water discharge (in terms of stream power)
2. Sediment load (amount and variations)
3. Fluvial and geological characteristics (soil strata and land use and land cover status)

Braided channels occur in rivers with steeper bed slope when threshold level of sediment load or slope is reached; any slope over this threshold creates a braided stream. This occurs due to rapid evaporation and infiltration after period of heavy rainfall. It can lead to deposition of sediment load. Braiding is caused by fluctuations in discharge levels and low river stream power with sufficient sediment particles.

The generation of stream power depends on the velocity, so the relationship between velocity and different types of sediment particle movement can evolve very promptly for the braiding river. Hjulström proposed one of the very important curves named as Hjulström curve (Fig. 9.12) to define erosion, transportation and deposition zones based on the velocity and type of particles.

The majority of theories and studies have been attempting to explain the reasons for braiding in a river system which involve establishing an empirical relationship between braiding and hydrological characteristics such as watershed area, discharge, channel or valley slope, sinuosity, width to depth, sediment supply, sediment particle size and bank resistance. Slope and water discharge can be quantified more readily and accurately than sediment supply and usually form the bases for empirical meander/braided thresholds.

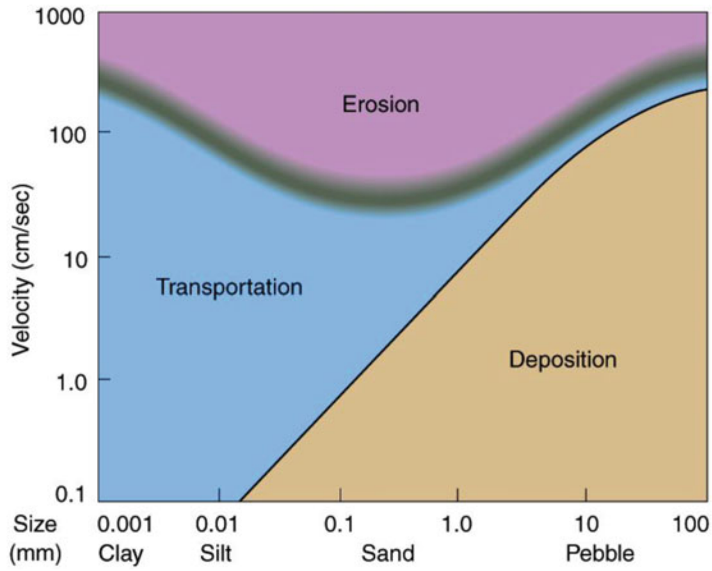

Fig. 9.12 Standard Hjulström curve (http://greenfieldgeography.wikispaces.com/Floodplain+management)

The understanding of the basic mechanisms operating the large-scale morphodynamics of river systems has been substantially improved in the last 50 years. The latter progress, though accomplished with the aid of a large number of field observations and laboratory investigations, is mainly the result of theoretical analyses based on a mechanical approach, coupled with reasonable assumptions on relative importance of the temporal and spatial scales involved. This part of the study involved with laboratory investigation of turbulence parameters under braided condition.

Alluvial river channels are self-formed as they flow over the alluvial lands having sandy-silty-clay materials. Their morphology results from the entrainment, transportation and deposition of the unconsolidated sedimentary materials of the valley fill and floodplain deposits across which they flow (Richards et al. 1993). In the natural condition, there are several river patterns such as a straight river, meandering river and braided river that exist. The structure of secondary current, bed shear stress in the meandering channel has been thoroughly studied by conducting the experiment and numerical simulation. Some research has been done to understand the turbulence characteristics of flow in the braided river; however, these works are not sufficient to fully understand the turbulence characteristics of flow around the braid bar (Murray and Paola 1994; Richardson and Thorne 2001; Roy and Bergeron 1990). A turbulent phenomenon in the braided river is much more complex than that in straight and meandering rivers, and turbulent flow characteristics around the braid bar are not well known till now (Ferguson 1993; Parker 1976).

Braided streams are associated with high stream power and unstable braid bars formed from sediments, which are often unvegetated. Braiding is the division of a single channel into two or more channel ways. Braiding river may be envisaged as a series of channel segments, which divide and rejoin around bars in a regular and repeatable pattern. Lane (1957) stated that a braided stream is characterized by ‘having a number of alluvial channels with bars or islands between meeting and dividing again and presenting from the air the intertwining effect of a braid’. Schumm and Lichty (1963) expressed the braided channels as single bedload rivers which at low water have islands of sediment or relatively permanent vegetated islands in contrast to multiple channels in which each branch may have its own individual pattern.

9.4.7.2 Causes of Braiding

Cause and effect of braid bar development is difficult to determine but Leopold and Wolman (1957) in their flume experiment reported that a bar of coarse sand diverts flow to cause bank erosion and positive feedback then accentuates bar development and widening. Miller (1958) noted that the adjustment of width is the inverse of behaviour at tributary junctions. Generally, high-energy stream may create braided channel patterns as a result of the instability of bedload transport in wide, shallow channel (Parker 1976). Parker (1976) also has given an interpretation of the criterion for braiding and characteristics scale of meandering rivers. Process-based explanations of mid-channel bar initiation and growth, based on observation of flow patterns and sediment dynamic downstream of channel confluences, have been proposed by Ashmore (1991) and Ashworth Philip (1996) on the basis of measurements in the flumes and in the streams. While the models of Ashmore (1991) and Ashworth Philip (1996) may explain why bifurcation is likely to occur immediately downstream of an anabranch confluence, processes are observed at the confluence-influence unit. However, this does not fully explain the initiation of braiding in a single channel.

If the results of analyses based on fluid mechanics are accepted, it follows that the bifurcation of a single channel that results from inherent instability in the flow and deposition of bed material load at the centre is driven by flow instability. That is, sediment plays an essential, but responsive role in the bifurcation process, if braiding is division of a single flow stream into two or more threads. Morphological bifurcation of the channel can, indeed, occur subsequently by one of the five mechanisms described by Ferguson (1993).

9.4.7.3 Characteristics of Braided Channel

A braided stream occurs in high-energy environments of large and variable discharges, heavy sediment load and steeper gradient with erodible banks. Braided streams are characterized by wide and shallow cross sections with random bar formations creating flow divisions. Sediment transport takes place over the bar surface while incisions in the lateral channels lower the water surface to expose the bar, which then dissected. The complex of islands is stabilized by vegetation in natural streams and experience further high stage sedimentation (Richardson and Thorne 2001). The distributary channels formed by braiding are less hydraulically efficient than parent single channels. Braided reaches are characterized by steeper slope for maintenance of stream power necessary for sediment transport. As per Smith (1974), general characteristics of braided stream deposits include abundant ripple and dune, cross stratification, thin lenticular shales, many intraclasts, thin sedimentary units indicating variable flow regimes and numerous cut-and-fill structures.

9.4.7.4 Braiding and Turbulence

Both turbulence and stream braiding are represented by a hierarchy of scales. In turbulence the objects constituting these scales are referred as eddies; for braiding the bar, the term is used analogously for all types of sediment islands, including the whole zoology of bar types described by the previous researchers. Turbulence and braiding both exhibit fractal behaviour within the hierarchy of scales (Berge et al. 1984; Kozioł 2015). Also, both types of system interactions between structures give rise to short-lived events (ejection and sweep in turbulence and confluences in braiding) that contribute disproportionately to the overall net transport (momentum in turbulence; sediment in braiding).

9.4.7.5 Characterizing Turbulence

Turbulent eddies create fluctuations in velocity, and these fluctuations represent the chaotic motion. Turbulent flow can be characterized by the statistical concepts, and theoretically velocity is assumed continuous and mean velocity is calculated by integration. However, in practice velocity records consist of discrete samples u_i and w_i; hence, mean velocity (longitudinal and transverse) is calculated by summation of all discrete velocities divided by the number of discrete velocity sample as shown in Eqs. (9.5) and (9.6):

$$\overline{u} = \frac{1}{N}\sum_{i=1}^{N} u_i \quad (9.5)$$

$$\overline{w} = \frac{1}{N}\sum_{i=1}^{N} w_i \quad (9.6)$$

$$u_i^{'} = u_i - \overline{u} \quad (9.7)$$

$$w_i^{'} = w_i - \overline{w} \quad (9.8)$$

The quadrant events depend on sign of Reynolds stress components (longitudinal and vertical fluctuation components – Eqs. 9.7 and 9.8).

9.4.7.6 Experimental Programme

The experiments were conducted at the River Engineering Laboratory, Department of Water Resource Development and Management, Indian Institute of Technology, Roorkee, India. The experiments were carried out in a flume 2.6 m wide, 1 m deep and 10 m long. Velocity is measured at 12 points around the island (as shown in Fig. 9.13) in a braided river model with the help of ADV. The ADV uses the principle of Doppler shift to measure the velocity of water in three dimensions. The device sends out a beam of acoustic waves at a fixed frequency from a transmitter probe. These waves bounce off moving particulate matter in the water, and three receiving probes 'listen' for the change in frequency of the returned waves. The ADV then calculates the velocity of the water in the x, y and z directions. A braided river model with a central island is constructed in the River Engineering

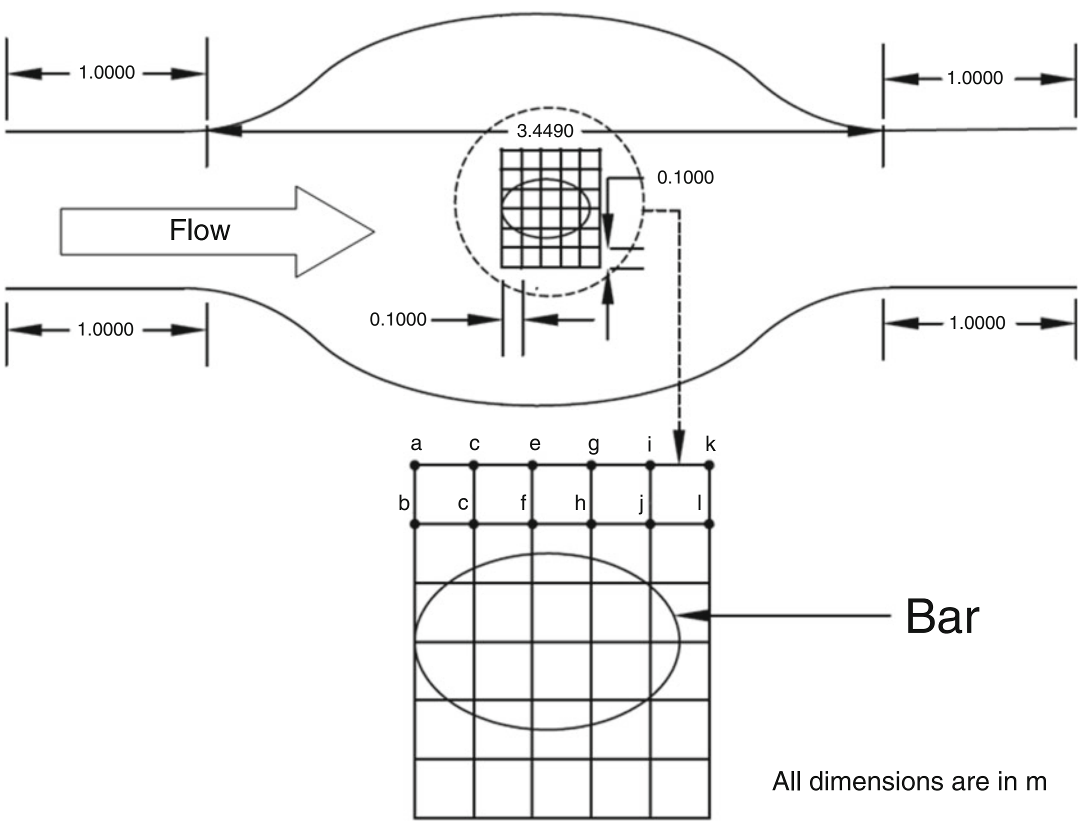

Fig. 9.13 Sketch of centrally braided river model

Lab, IIT, Roorkee. The flow characteristics are studied around central braided bar using quadrant analysis. The conventional quadrant method involves studying the relationship between temporal fluctuations of velocity components, u' and w', particularly their distribution between four quadrants numbered as shown in Table 9.2. u' and w' are fluctuating velocity components in longitudinal and vertical direction, respectively. These fluctuating velocity components are calculated using Eqs. (9.7) and (9.8). After studying the fluctuation behaviour of u′ and w′, it is found that turbulent phenomenon exhibits coherent structure. Experiments were carried out at two different water flow rate of 60,000 and 40,000 cm^3/s. The velocity was measured at the distance of 0.6 cm from the bed at these points. The scouring/deposition data are collected around the island at these selected 12 points for two different discharges (Fig. 9.13). The objective of this experimental programme is to relate the bursting ratio (a new defined parameter by the authors) to the deposition and scouring patterns around the island in a braided river model.

9.4.7.7 Analysis of Experimental Data

9.4.7.7.1 Conditional Probability

Based on two-dimensional velocity fluctuations, the probability of the occurrence of each quadrant bursting event is determined by Eqs. (9.9) and (9.10):

$$P_k = n_k/N \tag{9.9}$$

$$N = \sum_{k=1}^{k=4} n_k \tag{9.10}$$

where P_k is the probability of occurrence of the events belonging to quadrant k, n_k is the number of events belonging to k quadrant, and N is the total number of events. Using the equation given above, the probability of occurrence of sweep and ejection quadrant events was calculated at given points of flow within the depth. The conditional probability of occurrence of sweep and ejection quadrant events is calculated at 12 different points at the distance of 0.6 cm from the bed.

The contributions of coherent structure mainly ejection ($Q2$) and sweep ($Q4$) are intensively studied by the researcher. Nakagawa and Nezu (1977, 1978) and Grass (1971) have extensively studied quadrant events, and they found that sweep is the most important event that is related to transfer of momentum into the boundary layer. In addition, they found that frequency of sweep and ejection are more as compared to outward interaction ($Q1$) and inward interaction ($Q3$) events. A new turbulence parameter bursting ratio is defined in this study; it is defined as the ratio of probability occurrence of even events to the odd events. The bursting ratio is given by Eq. (9.11):

$$B_r = \frac{Q2 + Q4}{Q1 + Q3} \tag{9.11}$$

9.4.7.8 Results and Discussions

The bursting ratio has been found to be high at points of scouring, and their values are low at the points of deposition (Fig. 9.14), which also shows that the bursting ratio is related to the scouring/depositions around the bar. From Table 9.11, it has been encountered that the values of bursting ratios decreased when the discharge decreases from 60,000 to 40,000 cm^3/s. For discharge of 60,000 cm^3/s, the maximum value of bursting ratio is 2.92, and for 40,000 cm^3/s it was decreased to 2.52. This shows that the even events $Q2$ and $Q4$ weaken down by lowering the discharge. Since these events are primarily responsible for scouring around the island, thus lower discharge will enhance depositions around the island in the braided river model.

Analysis of scouring/depositional pattern with bursting ratio under braided river model (Fig. 9.14) discloses a remarkable point. The results constitute threshold point of bursting ratio, and it indicates that if the bursting ratio is greater than 1, chance of scouring at that point will be high, and if bursting ratio is less than 1, chance of deposition will be more. This may prove a better parameter for scouring/deposition under different hydraulic conditions.

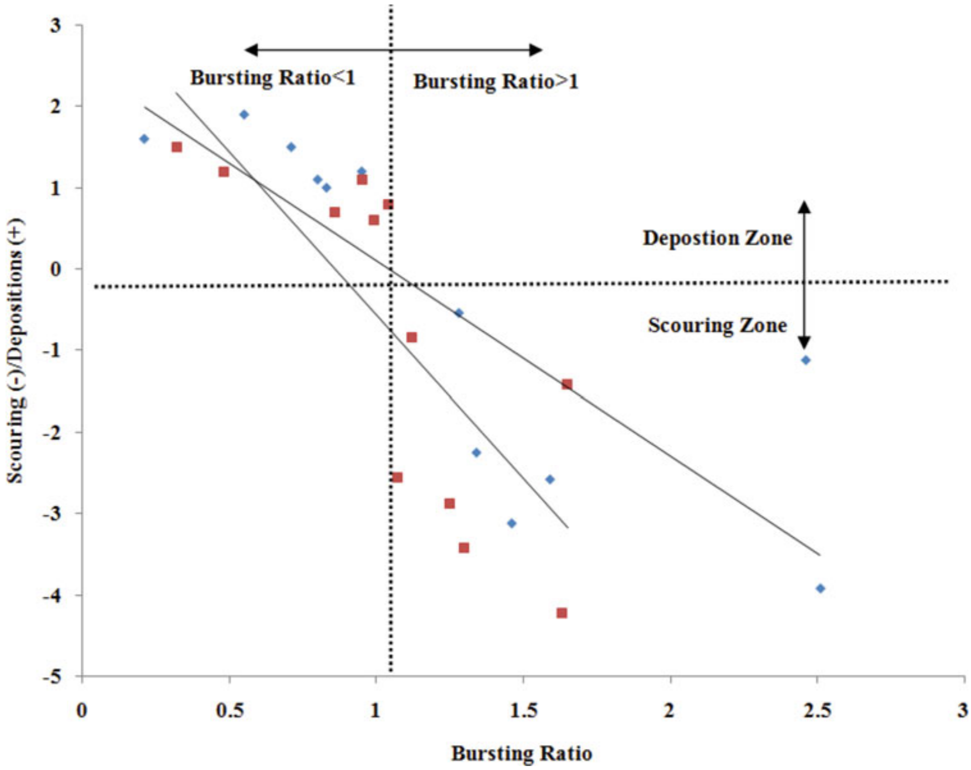

Fig. 9.14 Graph between scouring/depositions (cm) and bursting ratio

Table 9.11 Scouring and deposition patterns at different positions around bar

Point	Experiment A scouring/deposition	Experiment B scouring/deposition
a	−3.12	−3.42
b	−3.92	−4.22
c	−2.25	−2.55
d	−2.58	−2.88
e	−0.54	−0.84
f	−1.12	−1.42
g	+1	+0.6
h	+1.2	+0.8
i	+1.1	+0.7
j	+1.5	+1.1
k	+1.6	+1.2
l	+1.9	+1.5

9.4.8 Conclusions

The main aim of this chapter is to provide the idea of newer methodology to study the river dynamics. Under turbulence scale conditions, there is the enormous possibility to the river behaviour study under several hydraulic conditions experimentally. This study is supported by controlled laboratory investigations under the state-of-the-art methodological analysis.

In the first part of the study, turbulence behaviour of river has been investigated for steady and unsteady flow conditions. Bursting events (quadrant and octant) with their first-order transitional probability have been looked into. Transitional probability of diagonal bursting events has been found to be increased for unsteady flow condition under both the methodologies (quadrant and octant). Change of effect of unsteadiness in different planes has also been estimated, and it was found that transverse plane is the least affected with unsteadiness of flow. The larger sets of experiments under field conditions have been proposed to evaluate the better understanding of these events.

In the second part of the study, turbulence behaviour of river has been investigated for centrally braided river model. A new parameter named bursting ratio is proposed in this study. Bursting ratio has been compared with the scouring and deposition events around the braided bar. Authors have concluded that the parameter has potential to separate the scouring and deposition phenomenon based on threshold value of bursting ratio. Threshold value of bursting ratio was estimated as one in this case study. The further refinement is possible based on larger datasets and several field experimentations.

References

Ashmore PE (1991) How do gravel-bed rivers braid? Can J Earth Sci 28(3):326–341

Ashworth Philip J (1996) Mid-channel bar growth and its relationship to local flow strength and direction. Earth Surf Process Landf 21:123

Berge P, Pomeau Y, Vidal C (1984) Order within chaos, Wiley and Sons, NY

Blöschl G, Sivapalan M (1995) Scale issues in hydrological modelling: a review. Hydrol Process 9(3–4):251–290

Bradshaw P (2013) An introduction to turbulence and its measurement: thermodynamics and fluid mechanics series. Elsevier, Burlington

Church M (1995) Geomorphic response to river flow regulation: case studies and time-scales. Regul Rivers Res Manag 11(1):3–22

Church M, Ferguson R (2015) Morphodynamics: rivers beyond steady state. Water Resour Res 51(4):1883–1897

Ferguson R (1993) Understanding braiding processes in gravel-bed rivers: progress and unsolved problems. Geol Soc Lond Spec Publ 75(1):73–87

Grass AJ (1971) Structural features of turbulent flow over smooth and rough boundaries. J Fluid Mech 50(02):233–255

Gordon CM (1975) Sediment entrainment and suspension in a turbulent tidal flow. Mar Geol 18(1):M57–M64

Helder W, Ruardij P (1982) A one-dimensional mixing and flushing model of the Ems-Dollard estuary: calculation of time scales at different river discharges. Neth J Sea Res 15(3–4):293–312

Keshavarzi AR, Gheisi AR (2006) Stochastic nature of three dimensional bursting events and sediment entrainment in vortex chamber. Stoch Env Res Risk A 21(1):75–87

Keylock C, Hardy R, Parsons D, Ferguson R, Lane S, Richards K (2005) The theoretical foundations and potential for large-eddy simulation (LES) in fluvial geomorphic and sedimentological research. Earth Sci Rev 71(3):271–304

Keylock CJ, Lane SN, Richards KS (2014) Quadrant/octant sequencing and the role of coherent structures in bed load sediment entrainment. J Geophys Res Earth Surf 119(2):264–286

Kline S, Reynolds W, Schraub F, Runstadler P (1967) The structure of turbulent boundary layers. J Fluid Mech 30(4):741–773

Kozioł A (2015) Scales of turbulent eddies in a compound channel. Acta Geophys 63(2):514–532

Lane EW (1957) A study of the shape of channels formed by natural streams flowing in erodible material. US Army Engineer Division, Missouri River

Leopold L, Wolman M (1957) River channel patterns: braided, meandering, and straight: US Geological Survey professional paper 282-B., 1960, River meanders. Geol Soc Am Bull 71:769–794

Mianaei SJ, Keshavarzi AR (2008) Spatio-temporal variation of transition probability of bursting events over the ripples at the bed of open channel. Stoch Env Res Risk A 22(2):257–264

Miller JP (1958) High mountain streams: effects of geology on channel characteristics and bed material. State Bureau of Mines and Mineral Resources, New Mexico Institute of Mining and Technology, Albuquerque

Murray AB, Paola C (1994) A cellular model of braided rivers. Nature 371:54–57

Nakagawa H, Nezu I (1977) Prediction of the contributions to the Reynolds stress from bursting events in open-channel flows. J Fluid Mech 80(01):99–128

Nakagawa H, Nezu I (1978) Bursting phenomenon near the wall in open-channel flows and its simple mathematical model. Kyoto Univ Fac Eng Mem 40:213–240

Nepf H, Vivoni E (2000) Flow structure in depth-limited, vegetated flow. J Geophys Res Oceans 105 (C12):28547–28557

Parker G (1976) On the cause and characteristic scales of meandering and braiding in rivers. J Fluid Mech 76(03):457–480

Richards K, Chandra S, Friend P (1993) Avulsive channel systems: characteristics and examples. Geol Soc Lond, Spec Publ 75(1):195–203

Richardson LF (1921) Some measurements of atmospheric turbulence. Philos Trans R Soc Lond Ser A Cont Pap Math Phys Character 221:1–28

Richardson WR, Thorne CR (2001) Multiple thread flow and channel bifurcation in a braided river: Brahmaputra–Jamuna River, Bangladesh. Geomorphology 38(3):185–196

Roy A, Bergeron N (1990) Flow and particle paths at a natural river confluence with coarse bed material. Geomorphology 3(2):99–112

Schumm SA, Lichty RW (1963) Channel widening and flood-plain construction along Cimarron River in southwestern Kansas. US Geological Survey, Washington, DC

Seyfried M, Wilcox B (1995) Scale and the nature of spatial variability: field examples having implications for hydrologic modeling. Water Resour Res 31(1):173–184
Sharma N, Tiwari H (2013) Experimental study on vertical velocity and submergence depth near Piano Key Weir. Labyrinth Piano Key Weirs II-PKW 93–100
Smith ND (1974) Sedimentology and bar formation in the upper Kicking Horse River, a braided outwash stream. J Geol 82:205–223
Tiwari H, Sharma N (2014) Statistical study of turbulence near piano key weir: a review. J Exp Appl Mech 5(3):16–28
Tiwari H, Sharma N (2015a) Interaction between flow hydrodynamics and bed roughness in alluvial channel. ISH J Hydraul Eng 22(1):1–10
Tiwari H, Sharma N (2015b) Turbulence study in the vicinity of piano key weir: relevance, instrumentation, parameters and methods. Appl Water Sci 1–10
Whipple KX, Tucker GE (1999) Dynamics of the stream-power river incision model: implications for height limits of mountain ranges, landscape response timescales, and research needs. J Geophys Res: Solid Earth 104(B8):17661–17674

Harinarayan Tiwari Department of Water Resources Development and Management, Indian Institute of Technology Roorkee, Roorkee, Uttarakhand, India

Amir Khan Department of Water Resources Development and Management, Indian Institute of Technology Roorkee, Roorkee, Uttarakhand, India

Nayan Sharma Department of Water Resources Development and Management, Indian Institute of Technology Roorkee, Roorkee, Uttarakhand, India